

# ACCURACY OF GPS PRECISE POINT POSITIONING (PPP)

by

Simge TEKİÇ

B.S., Geodesy and Photogrammetry Engineering

Yıldız Technical University, 2006

Submitted to the Kandilli Observatory and  
Earthquake Research Institute in partial fulfillment of  
the requirements for the degree of  
Master of Science

Graduate Program in Geodesy

Boğaziçi University

2009

## ACKNOWLEDGEMENTS

This study becomes realized with many valuable contributions. Firstly, I would like to thank to my supervisor, Assist. Prof. Dr. D. Uğur ŞANLI for his great support, guidance and encouragement for this study.

We are grateful to NASA's Jet Propulsion Laboratory for providing the GIPSY OASIS II software and for satellite orbit and clock solution files. We also thank the Scripps Orbit and Permanent Array Centre (SOPAC) researchers for opening their archives to scientific activities worldwide.

My endless gratitude is to, Gönül DÜZGÜN, for her love and support. Making her proud is always motivating. Through her I extend my thanks to all my friends and KOERI Geodesy Department for their hospitality and friendliness.

## ABSTRACT

### ACCURACY OF GPS PRECISE POINT POSITIONING (PPP)

We tried to show how the accuracy of GPS varies with respect to observing session duration by using the method of GIPSY precise point positioning (PPP), and how the site's coordinates latitude, longitude and ellipsoidal height are affected.

We used eleven IGS sites scattered almost evenly across the earth. GPS data were obtained from SOPAC archives at <http://sopac.ucsd.edu/cgi-bin/dbDataBySite.cgi> in Rinex (Receiver Independent Exchange) format. Processing of the GPS data was achieved through the use of Jet Propulsion Laboratory's GIPSY OASIS II software and the application of "Precise Point Positioning" method (PPP) by Zumberge *et al.*, (1997). In addition, least squares (LS) analysis was used to model the accuracy of PPP.

Our study is based on the mathematical expression of Eckl *et al.*, (2001) in which the dependence of accuracy on observing session is expressed with  $T$ . GPS data were segmented into shorter sessions from 1 h to 24 h. For each segment a GPS solution was produced using the PPP routine. We used RMS values from sub-segments to model the accuracy of GPS PPP.

Results indicate that accuracy of GIPSY PPP depends only on the observing session  $T$ . Observing sessions shorter than 4 hour show dependency on latitude especially for the components longitude and ellipsoidal height. Using session length of 6 or more hours one can model the accuracy of GPS PPP with a simple formulation. Our results also indicate that prediction formulation for PPP is only slightly different from that of relative positioning formulation.

## ÖZET

### GPS DUYARLI NOKTA KONUM BELİRLEME DOĞRULUĞU

İnsanlık tarihinde bugüne kadar yapılmış en önemli gelişmelerden biri de şüphesiz Global konum belirleme sistemi (GPS) dir. Gelişen Teknoloji ile birlikte GPS kullanım alanlarını artmıştır. Buna bağlı olarak kullanıcılarının sürekli artması sonucu sistemden etkin olarak yararlanabilmek amacıyla uluslararası GPS kamuoyu birtakım standartlar koyma gereği duymuştur. Bu amaçla Uluslararası Jeodezi Birliği tarafından 1993 yılında Uluslararası GPS Servisi kurulmuştur.

Dünya üzerine dağılmış, IGS'e ait istasyon noktalarından oluşmuş bir GPS ağı mevcuttur. Bu GPS istasyonlarında toplanan veriler her gün IGS bünyesindeki Analiz Merkezlerine gönderilmekte, burada değerlendirildikten sonra sivil kullanıcılara sunulması için Küresel Veri Merkezlerinde (Global Data Centers) arşivlenmektedir.

Bu çalışmadaki amaç GPS bağıl konum belirlemede yapılan çalışmaların yanı sıra, mutlak konum belirleme ya da literatürdeki adıyla duyarlı nokta konum belirleme (Precise Point Positioning/PPP) yardımıyla IGS noktalarının konum doğruluklarını belirlemektir. Uygulama için IGS Gözlem Ağının, Avrupa Kıtası, Asya Kıtası, Amerika Kıtası, Afrika Kıtası'na yayılmış durumda bulunan farklı enlemlerde olmak üzere toplam on bir adet nokta seçildi.

Uygulamada noktalara ait 24 saatlik veriler 1, 2, 3, 4, 6, 8, 12 saatlik zaman dilimlerine bölünüp, Scripps Orbit and Permanent Array Centre (SOPAC)' tan 10 günlük veri indirilerek ve JPL' den alınan hassas yörünge bilgisi ile GIPSY 4.0 yazılımı kullanılarak değerlendirildi. Farklı enlemlerde bulunan IGS noktalarının gözlem süresine bağlı GPS doğruluk değişimi gözlemlendi.

Elde ettiğimiz deęerlendirmeler sonunda GIPSY mutlak konum belirleme doęruluęunun sadece gözlem süresine baęlı olduęu sonucu elde edildi. Dört saatten küçük gözlem sürelerinde boylam ve elipsoit bileşenleri için enleme baęlılık tespit edildi. Altı ve daha uzun gözlem süreleri için ise GPS mutlak konum belirleme doęruluęunu bir tek formülle modelleyebileceğimizi elde ettiğimiz anlamlı dengeleme katsayı deęerleri ile ispatladık.

## TABLE OF CONTENTS

|   |     |
|---|-----|
| ACKNOWLEDGEMENTS.....                                       | iii |
| ABSTRACT.....   | iv  |
| ÖZET .....  | v   |
| LIST OF FIGURES .....                                       | ix  |
| LIST OF TABLES.....   | x   |
| LIST OF SYMBOLS / ABBREVIATIONS.....                        | xii |
| 1. INTRODUCTION .....                                       | 1   |
| 2. LEAST SQUARES ESTIMATION.....                            | 3   |
| 2.1. Linearised Model .....                                 | 3   |
| 2.2. Design Matrix .....                                    | 4   |
| 2.3. The Least Squares Solution .....                       | 4   |
| 3. INTRODUCING HIGH PRECISION GPS GEODESY.....              | 5   |
| 3.1. High Precision Software.....                           | 5   |
| 3.2. Sources of Data and Information.....                   | 6   |
| 3.2.1. IERS: International Earth Rotation Service.....      | 6   |
| 3.2.2. IGS: International GPS Service for Geodynamics ..... | 7   |
| 4. EPHEMERIS .....  | 9   |
| 4.1. The Broadcast Ephemeris .....                          | 9   |
| 4.2. The Precise Orbit .....                                | 10  |
| 5. SOURCES OF GPS ERROR .....                               | 11  |
| 5.1. Geometric Dilution of Precision (GDOP).....            | 11  |
| 5.2. Clock Errors .....                                     | 12  |
| 5.2.1. Satellite Clock Error .....                          | 12  |
| 5.2.2. Errors in Satellite Orbit .....                      | 13  |
| 5.3. Atmospheric Errors .....                               | 13  |
| 5.3.1. Tropospheric Errors.....                             | 13  |
| 5.3.2. Ionospheric Errors .....                             | 15  |
| 5.4. The Ocean Loading.....                                 | 17  |
| 5.5. Atmospheric Loading .....                              | 18  |
| 5.6. Multipathing Errors .....                              | 18  |

|   |    |
|---|----|
| 5.7. Receiver Clock Errors .....                | 19 |
| 5.8. Antenna Phase Center Variation Error ..... | 20 |
| 6. PRECISE POINT POSITIONING .....              | 22 |
| 7. STUDY AREA & ANALYSIS OF GPS DATA .....      | 23 |
| 8. ACCURACY ANALYSIS .....                      | 45 |
| 9. CONCLUSIONS .....                            | 48 |
| REFERENCES .....                                | 49 |
| AUTOBIOGRAPHY .....                             | 52 |

## LIST OF FIGURES

|             |   |    |
|-------------|---|----|
| Figure 3.1. | IERS Product Centers .....  | 7  |
| Figure 3.2. | IGS reference stations (as of October 2006) .....                                       | 8  |
| Figure 5.1. | Dilution of Precision: (a) poor DOP, (b) good DOP .....                                 | 12 |
| Figure 5.2. | Microwave radiometer measurements of the wet delay during a warm<br>front passage. .... | 14 |
| Figure 5.3. | Ionosphere regions .....  | 15 |
| Figure 5.4. | Multipathing Errors .....   | 19 |
| Figure 7.1. | Chosen IGS Tracking Stations .....  | 25 |
| Figure 7.2. | Chosen IGS Tracking Stations .....  | 25 |
| Figure 7.3. | Chosen IGS Tracking Stations .....  | 26 |
| Figure 7.4. | RMS values for each station for latitude component .....                                | 40 |
| Figure 7.5. | RMS values for each station for longitude component .....                               | 43 |
| Figure 7.6. | RMS values for each station for ellip. ht component .....                               | 44 |

## LIST OF TABLES

|             |   |    |
|-------------|---|----|
| Table 7.1.  | IGS stations we use .....   | 24 |
| Table 7.2.  | Chi <sup>2</sup> / DOF value .....  | 27 |
| Table 7.3.  | Latitude coordinate files .....   | 28 |
| Table 7.4.  | Longitude coordinate files.....   | 28 |
| Table 7.5.  | Ellipsoidal Height coordinate files.....                                      | 29 |
| Table 7.6.  | BOGT RMS values for latitude, longitude, and ellipsoidal height .....         | 30 |
| Table 7.7.  | YELL RMS values for latitude, longitude, and ellipsoidal height.....          | 30 |
| Table 7.8.  | HARB RMS values for latitude, longitude, and ellipsoidal height.....          | 31 |
| Table 7.9.  | GUAM RMS values for latitude, longitude, and ellipsoidal height.....          | 31 |
| Table 7.10. | MCM4 RMS values for latitude, longitude, and ellipsoidal height .....         | 32 |
| Table 7.11. | MALI RMS values for latitude, longitude, and ellipsoidal height.....          | 32 |
| Table 7.12. | IRKT RMS values for latitude, longitude, and ellipsoidal height.....          | 33 |
| Table 7.13. | QUIN RMS values for latitude, longitude, and ellipsoidal height .....         | 33 |
| Table 7.14. | RIGA RMS values for latitude, longitude, and ellipsoidal height .....         | 34 |
| Table 7.15. | MORP RMS values for latitude, longitude, and ellipsoidal height.....          | 34 |
| Table 7.16. | SFER RMS values for latitude, longitude, and ellipsoidal height .....         | 35 |
| Table 7.17. | Sample of high correlation between latitude and height component .....        | 36 |
| Table 7.18. | The ordering of stations from small to high values.....                       | 37 |
| Table 7.19. | RMS values for each station for latitude component .....                      | 38 |
| Table 7.20. | RMS values for each station for longitude component.....                      | 41 |
| Table 7.21. | RMS values for each station for radius component .....                        | 43 |
| Table 8.1.  | Comparing accuracy prediction with the mean RMS of GPS PPP<br>solutions ..... | 48 |

|            |   |    |
|------------|---|----|
| Table 8.2. | Comparing our PPP results with online Auto-GIPSY results..... | 48 |
|------------|---|----|

## LIST OF SYMBOLS / ABBREVIATIONS

|       |   |
|-------|---|
| CORS  | Continuously Operating Reference Systems      |
| GPS   | Global Positioning System                     |
| IGS   | International GPS Service                     |
| RINEX | Receiver Independent Exchange                 |
| ITRF  | International Terrestrial Reference Frame     |
| ICRF  | International Celestial Reference Frame       |
| ICRS  | International Celestial Reference System      |
| ITRS  | International Terrestrial Reference System    |
| SOPAC | Scripps Orbit and Permanent Array Center      |
| ECEF  | Earth-Centered Earth-Fixed                    |
| JPL   | Jet Propulsion Laboratory                     |
| PPP   | Precise Point Positioning                     |
| RMS   | Root Mean Square                              |
| NASA  | National Aeronautics and Space Administration |
| GNSS  | Global Navigation Satellite System            |
| DOP   | Dilution of Precision                         |
| PDOP  | Position Dilution of Precision                |

## 1. INTRODUCTION

Precise GPS point positioning (PPP), as an alternative to differential GPS Surveying, employs only one GPS receiver. However, the positioning accuracy is affected from global disturbances in addition to other unmodelled errors and biases. It is free from the reference receiver, its measurements and also its corrections.

Unmodelled errors and biases are the Primary limitation of GPS point positioning. These are ionospheric and tropospheric delays, ephemeris errors, multipath error, satellite altitude error, atmospheric loading, ocean loading and residual satellite clock errors. With the help of the international GNSS service (IGS), precise satellite ephemeris and clock data were produced and its further improvement to the point positioning is worth to mention here.

High-precision GPS information is provided by continuously operating GPS tracking stations and data centers, under the auspices of the International GPS Service. The IGS provide crucial tracking data from their affiliated stations dispersed worldwide, high accuracy satellite orbit and clock data, Earth rotation parameters, a unified reference frame of station velocities and coordinates, and ionospheric information (IGS, 2003).

As seen from the above explanations, several factors to which the accuracy of GPS (Global Positioning System) depends on influence the results. In addition to above influences duration of observation session has an effect on the results.

Several studies have been performed to assess the effect of observing session duration on GPS solutions. First, Eckl *et al.*, (2001) processed ten days of GPS data from 1998 to determine how the accuracy of a derived three-dimensional relative position vector between GPS antennas depends on the chord distance between these antennas and the duration of the GPS observing session. Their results show that highly accurate positional coordinates can be obtained using CORS as control. Furthermore GPS accuracy does not depend on the baseline length which could be formed from the nearest CORS that might be

as far as 300 kilometers away. However, long observation session duration is the need to obtain high accuracy for positional coordinates.

Dogan (2007) analyzed the observations made in the Marmara Continuous GPS Network (MAGNET) to determine how the accuracy of derived relative positions of GPS stations depends on the baseline length and the duration of the observing session. The results of the study showed that highly accurate positional coordinates can be obtained using MAGNET in the Marmara region. Moreover, distance and observing session plays an important role in determining the accuracy of a GPS derived relative positioning. Since he used different software (BERNESE), he noted the results are also dependent on the software used for the processing.

Sanli and Kurumahmut (2008) performed a detailed study on how the accuracy of GPS positioning varies with respect to observing session duration in the presence of large height differences. Their findings reveal that large station height differences bias GPS solutions even if the relative troposphere between baseline points is estimated. In addition, the effect of the large station height difference needs to be considered as an additional constraint in GPS accuracy studies

Parallel to the earlier studies of determining GPS accuracy with differential (relative) positioning conventionally, in this study we evaluate the accuracy of GPS derived from precise point positioning. Before going through the GPS experiment, in the next section, the highlights of the accuracy analysis is provided. In the sections 3 and 4, high precision GPS and its components are given. Section 5 reviews GPS error sources which are important on the point positioning accuracy.

## 2. LEAST SQUARES ESTIMATION

### 2.1. Linearised Model

We solve the point positioning problem by first linearising the root mean square (RMS) values of each day of GPS data. In the familiar methods of least-squares analysis, the equation is often written using matrix symbols as:

$$b = Ax + V \quad (2.1)$$

where  $b$  is the vector of solution RMS values as input observations,  $A$  is the design matrix,  $x$  is the matrix of unknown coefficients as will be described below, and  $V$  is the residual vector.

The equation we used is the modified form of the standard error expression given by Eckl *et al.* (2001). Accuracy of a GPS solution as a function of  $T$  and  $\varphi$  can be given by

$$S(\varphi, T) = \sqrt{\frac{a}{T} + \frac{(b \times \varphi^2)}{T} + c + d \times \varphi^2} \quad (2.2)$$

where  $T$  is the observing session duration in hours and  $\varphi$  is the geodetic latitude. The unknown coefficients  $a$ ,  $b$ ,  $c$ , and  $d$  are estimated using least squares analysis. This is a general equation for all three position components latitude, longitude, and ellipsoidal height.

## 2.2. Design Matrix

The linear coefficients, contained in the “design matrix”  $A$ , are actually the partial derivatives of each observation (*i.e.* RMS error in our case) with respect to each parameter (or unknown coefficient) in the Equation (2.2), computed using the provisional parameter values (Blewitt, 1997). The coefficients of  $A$  can be derived by partial differentiation of the observation equations.

## 2.3 The Least Squares Solution

Estimated residuals are the estimated model for the observations. Moreover, they are defined as the difference between the actual observations and the new ones. The estimated residuals can be given with the equation:

$$V = b - Ax \tag{2.3}$$

With the help of computing the value of  $x$  we can find the “least squares” solution. In fact we try to minimize the sum of squares of the estimated residuals. The following illustrates the application of this method to derive the least squares solution:

$$X = (A^T A)^{-1} A^T b \tag{2.4}$$

$x$  matrix expresses the unknown correction to the parameters. These are  $a, b, c, d$  in the equation (2.2) we used which given by Eckl *et al.* (2001). For further details of LS analysis of GPS solutions for the accuracy determination, the reader might refer to Eckl *et al.* (2001).

### 3. INTRODUCING HIGH PRECISION GPS GEODESY

#### 3.1. High Precision Software

Since the 1980's many software packages have been developed such as, BERNESE software, developed by the Astronomical Institute, University of Berne, Switzerland; GAMIT software, developed by the Massachusetts Institute of Technology, USA; GIPSY software, developed by the Jet Propulsion Laboratory, California Institute of Technology, USA. They are capable of obtaining high precision GPS positioning solutions for the point or points under consideration.

We processed our GPS data using GIPSY - OASIS (GOA II). It is an automated, fast, ultra-precise high precision GPS data processing software package for Precise Point Positioning (PPP) rather than relative positioning (Zumberge *et al.*, 1997). It overcomes the need for a base station in developing GPS applications. In GIPSY both the precise ephemeris and clock parameters are fixed by Jet Propulsion Laboratory (JPL).

Typical features of such software include:

- Orbit integration with appropriate force models;
- Accurate observation model (Earth model, media delay...) with rigorous treatment of celestial and terrestrial reference systems;
- Reliable data editing (cycle-slips, outliers);
- Estimation of all coordinates, orbits, tropospheric bias, receiver clock bias, polar motion, and Earth spin rate;
- Ambiguity resolution algorithms applicable to long baselines;
- Estimation of reference frame transformation parameters and kinematic modeling of station positions to account for plate tectonics and co-seismic displacements (Blewitt, 1997).

The typical quality of geodetic results from 24 hours of data can be summarised:

- Relative positioning at the level of few parts per billion of baseline length;
- Absolute (global) positioning at the level of 1 cm in the IERS Terrestrial Reference Frame (ITRF);
- Tropospheric delay estimated to a few mm
- GPS orbits determined to 10 cm;
- Earth pole position determined to 1 cm;
- Clock synchronization (relative bias estimation) to 100 ps (Blewitt, 1997).

## **3.2. Sources of Data and Information**

### **3.2.1. IERS: International Earth Rotation Service**

The IERS was established as the International Earth Rotation Service in 1987 by the International Astronomical Union and the International Union of Geodesy and Geophysics and it began operation on 1 January 1988.

The Central Bureau located at the Paris Observatory, France is responsible for the general management of the IERS consistent with the directives and policies set by the Directing Board. The Product Centres shown in Figure 3.1 are responsible for the products of the IERS. Products are Earth Orientation Data, Conventions, ICRF, ICRS, ITRF, ITRS and Geophysical fluids data. In our study, PPP results were computed using the International Earth Rotation Service's reference system ITRS (McCarthy *et al.*, 2003), as realized through the reference frame ITRF2005 (Altamimi *et al.*, 2007).



Figure 3.1. IERS product centers (IERS, 2009)

### 3.2.2. IGS: International GNSS Service for Geodynamics

We can think of the IGS as the highest-precision international civilian GPS community. The IGS is a voluntary federation of many worldwide agencies that pool resources and permanent GNSS station data to generate precise GNSS products (NASA, 2009).

Central Bureau located at the Jet Propulsion Laboratory, USA is responsible for the general management of the IGS and documented IGS Standards for permanent GPS stations. The International GNSS Service (IGS) provides Global Navigation Satellite Systems (GNSS) orbits, tracking data, and other high-quality GNSS data and data products on line in near real time. It oversees operation of global GPS network shown in Figure 3.2 (~340 stations) and maintains on-line database with Internet access.

The difference between "IGS data" and IGS products is that by "data" we mean raw GPS/GLONASS pseudorange and phase observations, broadcast ephemerides, and supporting types of raw data such as meteorological measurements. We use the term "products" for things like precise orbit and clock files, which are generated through



## 4. EPHEMERIS

An ephemeris as defined is a table giving the coordinates of a celestial body at a number of specific times within a specific period. As a surveyor we use ephemerides for position determination. We define our positions relative to GPS satellites. Therefore the need for an ephemeris plays an important role. Because, we need to know where the satellites are at a given time. As surveyors we accept GPS satellites as artificial stars. The broadcast ephemeris and the precise ephemeris are two general types.

### 4.1. The Broadcast Ephemeris

The broadcast ephemeris refers to broadcast from the GPS satellites. Relative to the WGS 84 datum we compute the earth\_centered earth\_fixed (ECEF) coordinates of each satellites. It consists Keplerian orbital elements which allow the computation by GPS receivers. Because they contain positional information. Daily dissemination of the broadcast ephemeris to the satellites is attained by the Control Segment (Langley, 1991).

The broadcast ephemerides for each GPS satellite are available in a RINEX-like file format while we collected GPS data. Since the precision of Broadcast ephemeris is not sufficient for our analysis (*i.e.* for precision work), we used Jet Propulsion Laboratory's precise ephemerides for producing our GPS solutions.

## 4.2. The Precise Orbit

Whereas the broadcast ephemeris contains information, *i.e.* the ECEF coordinates for each satellite relative to the WGS84 datum, the Precise Orbit contains information relative to the International Terrestrial Reference Frame (ITRF). In addition to this, the Precise one includes clock corrections. Moreover, at regular epoch intervals of 15 minutes this information is given for each satellite.

GPS satellite precise ephemerides (GPS orbits and clock corrections) are computed from the data collected at the IGS stations around the world. Replacing GPS's broadcast ephemerides with precise ephemerides improves GPS positioning accuracy (Heflin, 2009).

The IGS collects, archives, and distributes GPS and GLONASS observation data sets of sufficient accuracy to meet the objectives of a wide range of scientific and engineering applications and studies. These data sets are analyzed and combined to form the IGS precise orbits. (Menge, 2008).

We use the GPS analysis software GIPSY and hence it is compatible with Jet Propulsion Laboratory (JPL) products (*i.e.* precise clocks, orbits, and earth orientation parameters). Both the precise ephemeris and clock parameters are fixed by Jet Propulsion Laboratory (JPL), USA. We adopted the IGS precise orbits to achieve cm-level accuracy for our GPS data. Precise orbits were downloaded from JPL's ftp archives, which is one of the IGS analysis centers. In GIPSY analysis precise orbits can be downloaded using a command line `fetch_orbits` from directly JPL's data servers.

## 5. SOURCES OF GPS ERROR

In GPS analysis, in order to achieve accuracy to within a cm or better, extra efforts are necessary. Different sources can contribute to the total error in GPS measurements. As would be expected, a variety of different errors can occur within the system, some of which are natural, while others are artificial.

Unlike in relative positioning, common mode errors do not cancel in PPP. Our stations under consideration contain errors which need to be removed. These are satellite dependent errors including GDOP, clock error, orbit error & SA (removed on May 1, 2000), propagation dependent errors including Ionosphere, troposphere, multipath, and, receiver dependent errors including receiver clock error, antenna phase centre variation, and measurement uncertainty (King *et al.*, 2002).

### 5.1. Geometric Dilution of Precision (GDOP)

To improve the positioning accuracy in GPS point positioning, the geometric dilution of precision (GDOP) is commonly considered. DOP values are reported in three types of measurements: horizontal, vertical, and mean. Horizontal DOP (or HDOP) measures DOP as it relates to latitude and longitude. Vertical DOP (or VDOP) measures precision as it relates to altitude. Mean DOP, also known as Position DOP (PDOP), gives an overall rating of precision for latitude, longitude and altitude. Each DOP value is reported as a number between one and fifty where fifty represents very poor precision.

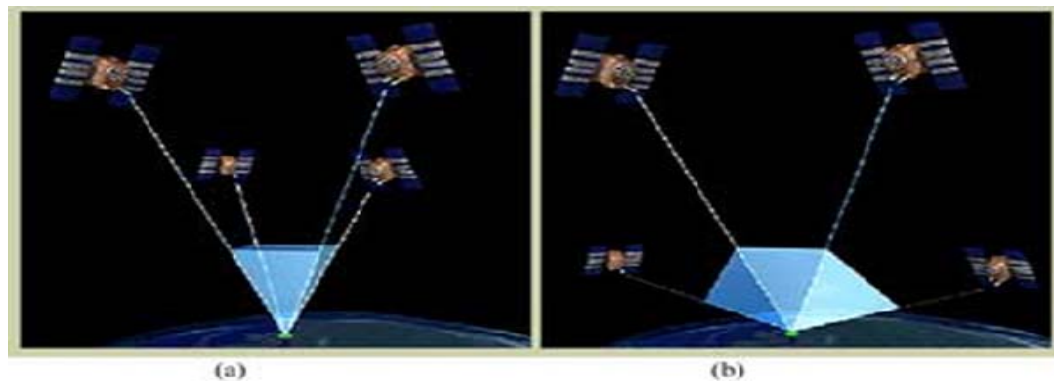


Figure 5.1. Dilution of precision: (a) poor DOP, (b) good DOP  
(Blewitt, G., 1997).

## 5.2. Clock Errors

### 5.2.1. Satellite Clock Error

It is caused by inability of satellite oscillator (clock) to maintain the GPS time. GPS satellites use high stability atomic clocks (caesium or rubidium), which result in satellite clock errors which are smaller than receivers because they use cheaper crystal oscillators (clocks).

Satellite clock errors are broadcasted by the navigation message. So, the satellite clock errors can be modelled using the broadcast satellite. Clock corrections can be removed using the single differencing.

In this study, we use JPL's precision satellite clock estimations. They are downloaded from JPL's ftp site [sideshow.jpl.nasa.gov](ftp://sideshow.jpl.nasa.gov) and used as input in GIPSY processing.

### **5.2.2. Errors in Satellite Orbit**

GPS satellites are affected from various disturbances through their travel in their orbits. These are mainly gravitational affects of the planets, air drag/friction, solar winds and pressure, etc. These effects are very well modeled by JPL and included in the precise orbits in .eci format. They could also be downloaded from JPL with the other products during the processing.

## **5.3. Atmospheric Errors**

The speed of light is computed based on a propagation through a vacuum (299 792 458 m/second). Propagation through the atmosphere causes changes the speed of the satellite signal. In order to control the atmospheric errors, an elevation mask is adopted during data collection and processing (eg. 10-15 degrees). In our processing, we chose the elevation angle as 15 degree. GPS signals are mainly affected from two types of atmospheric effects; tropospheric error and ionospheric errors (Yavasoglu, 1997).

### **5.3.1. Tropospheric Errors**

The electrically neutral atmosphere acts as a non-dispersive medium at the radio frequencies used by the GPS, and is responsible for both retardation in the propagation speed and ray bending. The effect of the electrically neutral atmosphere is usually referred as troposphere delay, as the troposphere accounts for most of the delay (Mendes and Langley, 2000).

Troposphere causes a delay on code & carrier measurements which may reach about 2.5 metres at the zenith & 30 meters at the horizon. The delay varies with temperature, pressure, humidity & the height of the receiver. The error has two parts: dry & wet components. Dry component can be modelled with the surface measurements. However, it is difficult to model the wet component in this way due to the difficulties in estimating water vapour content. Water Vapour Radiometer (WVR) can be used to model the wet component as shown in Figure 5.2. The total lack of correlation between the delay obtained

from the ground based model (Saastamoinen, 1972) and the delay estimates from the radiometer.

The models used in tropospheric modeling are

- Hopfield
- Black
- Saastamoinen
- Modified Hopfield

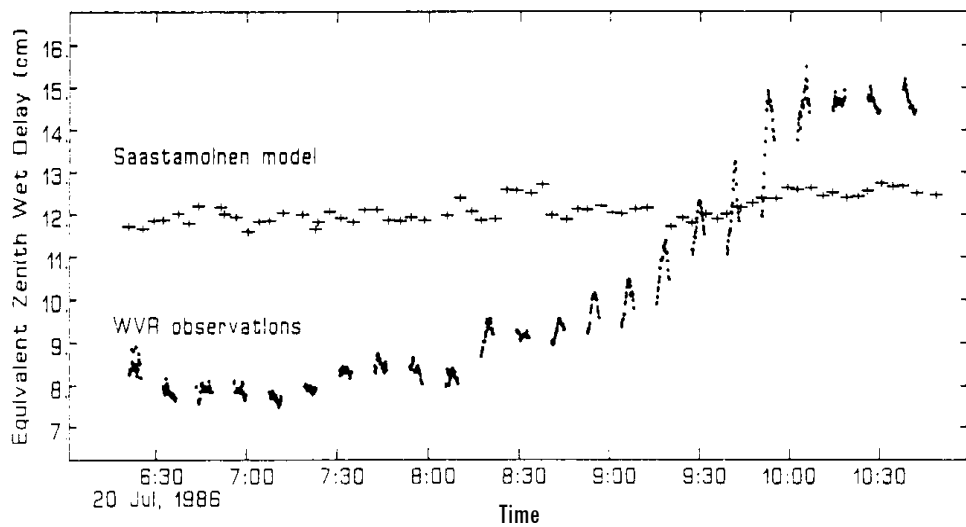


Figure 5.2. Microwave radiometer measurements of the wet delay during a warm front passage.

GIPSY processing uses stochastic modeling of the troposphere. The statistical model random walk is used to reveal the time variation of the instant tropospheric zenith delays. The process noise used in the estimation is  $1\text{cm}/\sqrt{h}$  where  $h$  is the hour.

### 5.3.2. Ionospheric Errors

Free thermal electrons are present in the ionosphere. The number of free electrons is defined by the Total Electron Content (TEC). The TEC varies with a number of factors including time of day, location, season, and also the period of the 11 year sunspot cycle. In Figure 5.3, the altitude of the ionosphere is illustrated from the earth surface. Ionospheric errors can be eliminated using dual frequency receivers (L1 & L2). The resulting phase (L3) is called ionosphere-free linear combination. For single frequency receivers, the measurements should be modelled and the receiver separations should be kept as short as possible (Witchayangkoon, 2000).

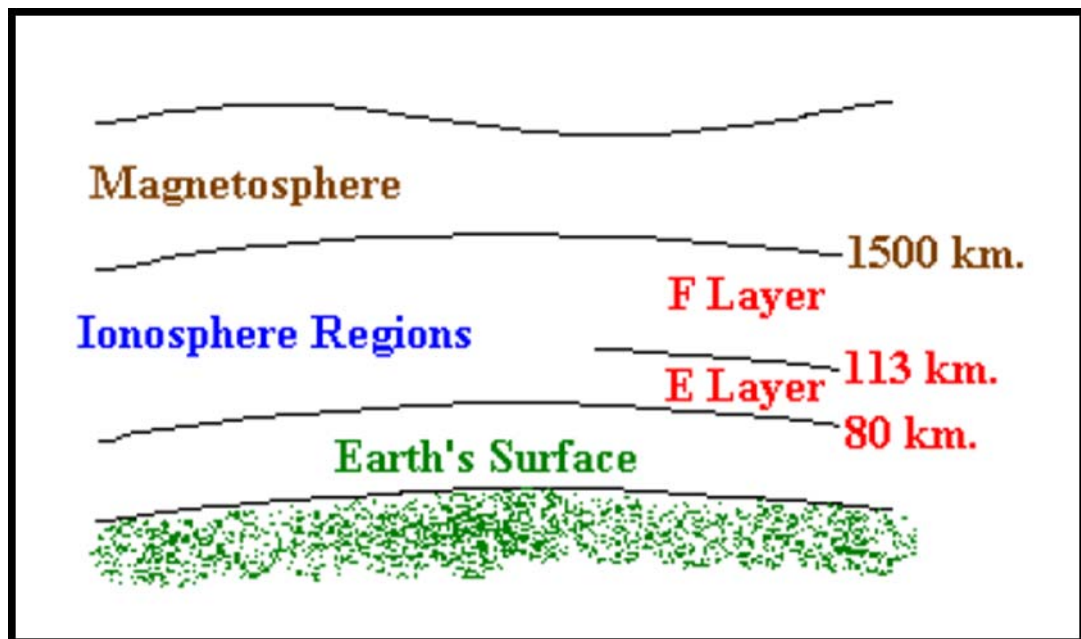


Figure 5.3. Ionosphere regions (Witchayangkoon, 2000).

The magnetosphere refers to the outermost region where the particle motion is controlled by the geomagnetic field. There are two distinct regions in the nomenclature of ionization as shown in Figure 5.3 The ionosphere can be divided into two main layers called the E layer (sometimes called the Heaviside layer or Kennelly-Heaviside layer, from about 80 to 113 km.) and the F layer (sometimes called the Appleton layer, which is above the E layer). The E layer reflects low frequency radio waves while the F layer reflects higher-frequency radio signals. The F layer is composed of two layers: the F1 and F2 layers, which start approximately at 180 and 300 km above the Earth's surface, respectively. The thickness of the F layer changes at night, thus altering its reflecting characteristics (Jursa, 1985).

This effect varies with the square of frequency  $f$  of the signals. We tried to eliminate this effect by having dual-frequency observation from our observation data.

In GIPSY processing, the ionospheric effect is eliminated using the data combination of L1 and L2 frequencies over both carrier phase observations and pseudo-range observations. However, we suspect this modeling leaves second order ionospheric effects on the solutions derived from short observation sessions. This will be described in the upcoming sessions.

#### 5.4. The Ocean Loading

It is known that elastic response of the Earth's crust to ocean tides affects the positioning. The movements caused by the ocean loading are more pronounced in oceanic and coastal areas. Tidal processes are described to a very high order of approximation by sinusoidal variations in time. Only a few coefficients need to be imported into fairly unsophisticated formulas in order to describe tidal motion for extensive time periods (Scherneck and Bos, 2000).

Ocean loading, *i.e.* primarily vertical variation of the crust in primarily coastal areas, is caused by sea level fluctuations due to the tides. In order to achieve truly centimeter-level global geodesy, ocean loading must be included in the site positional analysis (Witchayangkoon, 2000).

The conventional IERS models to compute ocean loading displacements (IERS Conventions, 1996) do not include the motion of the origin of the coordinate system (motions 45 of the center of mass), but contain only the displacements due to deformation with respect to the center of gravity of the solid earth (Scherneck, 1998a).

Ocean tide loading is the largest perturbation in the solid Earth tide predictions. Both amplitude and phase of ocean loading effects are heavily station and frequency dependent, normally having magnitude of centimeters, and where the vertical displacement is approximately three times larger than the horizontal components (Witchayangkoon, 2000).

Processing our GPS data, we modeled the effect of ocean tide loading using the using web based "Ocean Tide Loading Provider" developed by Bos and Scherneck (2000).

### 5.5. Atmospheric Loading

Today GPS (Global Positioning System) observations are used routinely for geodetic and geophysical experiments. Recently, research results using IGS (International GPS Service) data reveals that GPS observations contain periodic (geophysical) signals due to the loading effect of the atmosphere (Van dam *et al.*, 1994, Blewit, 1994).

It has long been acknowledged that atmospheric pressure loading (ATML) causes deformation of the surface of the Earth. Especially the GPS stations at higher latitudes and the vertical component are affected. The effect of Atmospheric loading is almost eliminated if continuous GPS data is used or GPS campaigns are extended over 2-week period (Blewitt, 1994). Since we used 10-day continuous GPS data for this study, we assume the effect of the atmospheric loading was largely eliminated. Correlating latitude values to RMS errors also reveal that, the effect of atmosphere loading is not encountered at higher latitudes (especially on the station YELL).

### 5.6. Multipathing Errors

The term multipath is derived from the fact that a signal transmitted from a GPS satellite can follow a ‘multiple’ number of propagation ‘paths’ to the receiving antenna. This is possible because the signal can be reflected back to the antenna off surrounding objects, including the earth’s surface (Townsend *et al.*, 1995).

Some important characteristics of multipath shown in Figure 5.4 are as follows (Townsend and Fenton, 1994):

- The multipath signal will always arrive after the direct path signal because it must travel a longer propagation path.
- The multipath signal will normally be weaker than the direct path signal since some signal power will be lost from the reflection. It can be stronger if the direct path signal is hindered in some way.
- If the delay of the multipath is less than two PRN code chip lengths, the internally generated receiver signal will partially correlate with it. If the delay is greater than 2

chips, the pseudorandom (PRN) codes are designed so that correlation power will be negligible.

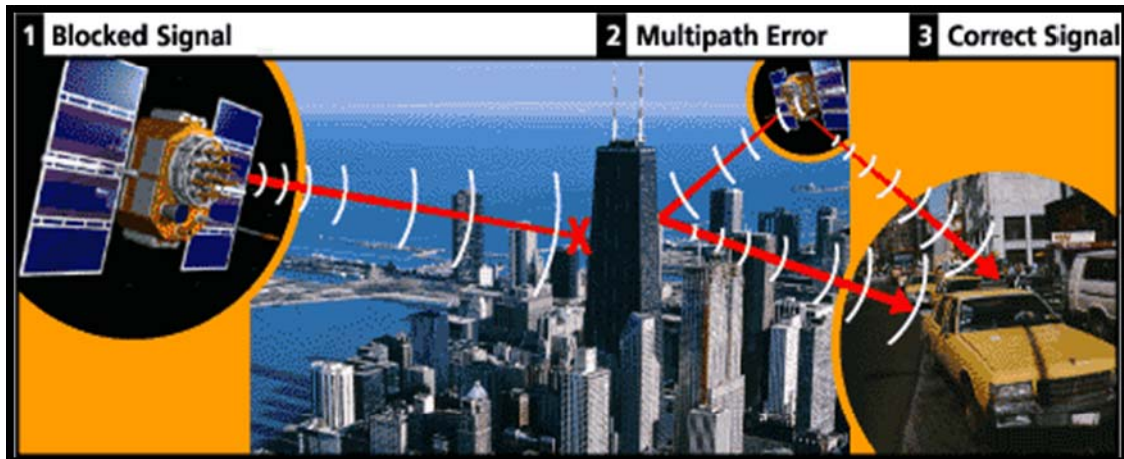


Figure 5.4. Multipathing errors (Stewart, 1998)

In our GPS analysis, we did not perform a thorough multipath elimination procedure however we know that IGS standards require the GPS stations employ the antennas that are highly protective against multipath. Most of them use choke-ring antennas in which the signals that are reflected from the ground are totally eliminated.

### 5.7. Receiver Clock Errors

Receivers use inexpensive quartz crystal source. The reason is to keep the receiver costs to an affordable level. The receiver clock error is larger than the satellite clock errors. If the receiver clock is in error, the error will affect all the measurements to all satellites. The receiver clock error is identical for all satellites observed simultaneously. To determine the 3D position, three unbiased satellites measurements are required. To account for the receiver clock error, an additional satellite is observed.

In GIPSY processing, the receiver clock error is estimated as an additional parameter using pseudo ranges. When necessary an iterative procedure is used so that the coordinates will approach to a trash-holder value.

### **5.8. Antenna Phase Center Variation Error**

In a GPS receiver antenna, the phase centre is the point in the antenna at which the GPS signals physically arrive. A relative GPS carrier phase solution effectively measures the vector between the phase centres of two antennae situated at either end of a baseline. To relate this vector to physical points on the ground, the exact location of the phase centre of each antenna relative to those points must be known (Stewart, 1998).

Changes in the orientation of one antenna create phase differences, which are completely independent from the antenna used at the reference site of the baseline. The phase differences, which originate from the antenna can therefore be used to model phase center variations. The phase center variation signal represents errors, which are introduced by neglecting the orientation of two antennas (Wübbena, 1997). Phase centre errors can be particularly important for applications requiring high resolution in the height component, such as tide gauge monitoring or GPS geoid determination (Stewart, 1998).

In GIPSY processing, we use a database (pcenter) that contains phase center variations for various types of the GPS antennas. When using it offsets caused using different brands of GPS antennas are taken into account in the processing.

## 6. PRECISE POINT POSITIONING

NASA's Jet Propulsion Laboratory scientists developed PPP which is a new high precision mode of GPS positioning (Zumberge *et al.*, 1997). It provides less than 1 cm accuracy with single receiver and without any ground control. PPP should not be confused with average point positioning which is performed in real time using pseudo ranges, and gives about 5-10 m precision (Sanli, 1999).

The main idea basing PPP idea is that we have precise orbits and clock information from some other source we can position ourselves (along with receiver clock and tropospheric bias) very accurately. IGS provides accurate orbits and clocks from a global network of GPS stations. For predicting precise orbits and clocks at least twenty or more stations are used and adding one extra station would only do a little change in the orbit estimation. So we can consider a user's receiver coordinates as the local parameters and take the global solution to be one using the current global network (Sanli, 1999).

The vast majority of commercially available software utilizes the principles of relative positioning. However, in the late 1990s, the Jet Propulsion Laboratory (NASA) pioneered a new technique that did not require differencing to obtain precise positions. They labeled it Precise Point Positioning (PPP) and implemented it in their GIPSY/OASIS II GPS processing software (King *et al.*, 2002).

The largest difference between relative processing and PPP is the way that the satellite and receiver clock errors are handled. Instead of between-receiver differencing to remove the satellite clock errors, PPP uses highly precise satellite clock estimates. These satellite clock estimates are derived from a solution using data from a globally distributed network of GPS receivers (King *et al.*, 2002).

We have to deal with unmodelled errors, namely tropospheric delay, satellite attitude error, and site displacement effect to achieve the highest possible point positioning accuracy. Moreover, we used precise ephemeris from JPL and satellite clock data produced by the International GPS Service.

## 7. STUDY AREA & ANALYSIS OF GPS DATA

Employing as research software, GIPSY is automatic and requires the user to input observation files for professional users. Here the GIPSY 4.0 is used with precise ephemeris obtained from Jet Propulsion Laboratory. IGS stations which are BOGT, IRKT, MORP, SFER, GUAM, MALI, QUIN, YELL, HARB, MCM4, RIGA shown in Table 7.1 and Figure 7.1-3 were chosen as stations under consideration.

GPS data including the 3-D coordinates of stations were provided in ITRF 2005 at an epoch of 1995.00, SOPAC archives at <http://sopac.ucsd.edu/cgi-bin/dbDataBySite.cgi> in Rinex (Receiver Independent Exchange) format. GPS data were sampled with 15 degree elevation cut off and 30 second recording intervals. It should be pointed out that IGS precise ephemeris is also referred to the ITRF reference system (El-Rabbany, 2002). For each station, we selected consecutive ten days of data observed during January 2008 and paid attention for observation files in that consecutive days should not contain a missing data.

Table 7.1. IGS stations we used

| Site ID | Site Name                | Country                     | Lat(m)       | Lon (m)       | Ellip. Ht (m) |
|---------|--------------------------|-----------------------------|--------------|---------------|---------------|
| BOGT    | Bogota                   | Colombia                    | 4.64007343   | -74.08093952  | 2576.5139     |
| YELL    | Yellowknife              | Canada                      | 62.48089338  | -114.48070296 | 180.9175      |
| HARB    | Hartebeest-<br>hoek      | Republic of<br>South Africa | -25.88696215 | 27.70724533   | 1558.0911     |
| GUAM    | USGS Guam<br>Observatory | Guam                        | 13.58932947  | 144.86836073  | 201.9283      |
| MCM4    | McMurdo<br>GPS Station   | Antarctica                  | -77.83834982 | 166.66933012  | 97.9642       |
| MALÌ    | Malindi                  | Kenya                       | -2.99591     | 40.1944       | -23.3382      |
| IRKT    | IRKUTSK                  | Russia                      | 52.21902398  | 104.31624201  | 502.3539      |
| QUIN    | Quincy                   | USA                         | 39.97455399  | -120.9444298  | 1105.7748     |
| RIGA    | RIGA<br>permanent<br>GPS | Latvia                      | 56.94862021  | 24.05877515   | 34.7264       |
| MORP    | Morpeth                  | England                     | 55.21279093  | -1.68549527   | 144.4531      |
| SFER    | San<br>Fernando          | Spain                       | 36.46434617  | -6.20564492   | 84.1759       |



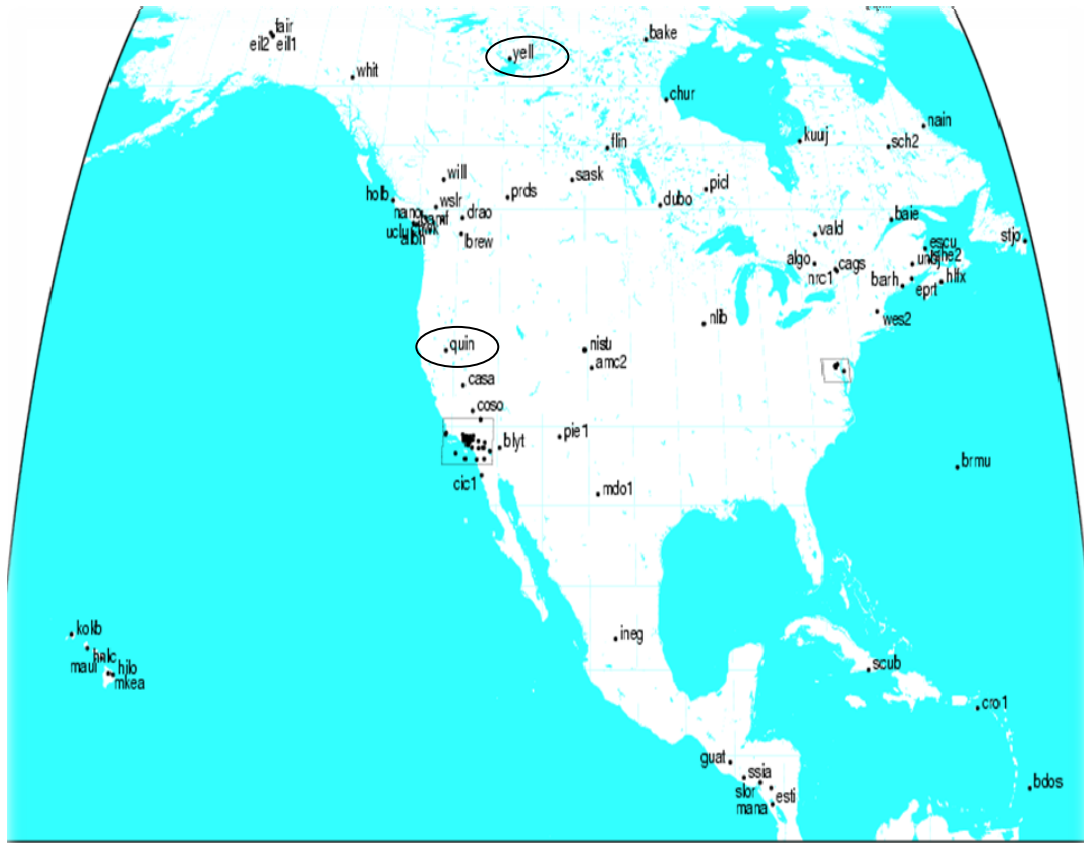


Figure 7.3. Chosen IGS tracking stations

Atmospheric loading has almost been eliminated since we used 10-day continuous data. Ionospheric influences were removed by the use of dual frequency receivers employed in IGS stations.

We downloaded the files in a z compressed format, such as bogt0050.05d.z then we tried to make an evaluation of a ten-day data by using the point\_rnx (precise point positioning) module of GIPSY. With the help of point\_rnx, we obtain three files including stacov files in ITRFxx and log files. stacov files include the final solution in X, Y, Z. On some occasions, we have to use the `-force` command to obtain a solution. However, in this case, free sta\_cov, free ITRFxx and free log files are produced. The force solution may be untrustworthy. Moreover, we wrote simple scripts which execute recursive processing.

Then we subdivided each day's data into non overlapping sessions for each selected value of  $T$  such as 1, 2, 3, 4, 6, 8, 12, 24 hours. With the help of other utility scripts GIPSY, time series results from sub-divided sessions were combined and analysed.

In some occasions, we use  $vi$  operator to correct dates. With the help of scripts we determined the ratio  $\chi^2/\text{DOF}$  that indicates the quality of processing. If it is around 1 the processing is successful, if it is fairly large the solution is most likely to appear as an outlier. In Table 7.2, we present  $\chi^2/\text{DOF}$  for the processing of the IGS stations used in the study. Note that the value of  $\chi^2/\text{DOF}$  is fairly large for HARB. When outliers from the processing were removed, the  $\chi^2/\text{DOF}$  value approached to 1.

Table 7.2.  $\chi^2/\text{DOF}$  values for the processing of the IGS stations used

| Site ID | $\chi^2/\text{DOF}$ | n    | e    | U    |
|---------|---------------------|------|------|------|
| GUAM    | 156,10              | 3,72 | 0,33 | 1,27 |
| QUIN    | 6,55                | 0,42 | 0,34 | 0,86 |
| HARB    | 2,70                | 0,23 | 0,19 | 0,07 |
| IRKT    | 1,28                | 0,31 | 0,08 | 0,65 |
| MALI    | 3,42                | 0,43 | 0,20 | 0,95 |
| MCM4    | 3,51                | 0,41 | 0,28 | 0,79 |
| MORP    | 1,63                | 0,20 | 0,20 | 0,47 |
| SFER    | 8,87                | 0,66 | 0,26 | 1,66 |
| YELL    | 11,79               | 0,12 | 0,16 | 0,73 |

Here subdivision for mutually non\_overlapping sessions was performed for  $T$  (1, 2, 3, 4, 6, 8, 12, 24) then we carried out the separation of 3-D coordinates. To separate latitude, longitude and radius in Matlab, ellipsoidal height components `gip2mat_gd.M` file was used. Figure 7.3 - Figure 7.5 comprise sample coordinate files following the separation for 24 hours data. As an important point, Matlab produces files in a Unix format but we need to change them into ascii format to evaluate our results in Excel.

Table 7.3. Latitude coordinate files

| Site ID | Date    | Latitude (°) | Formal Error (m) |
|---------|---------|--------------|------------------|
| HARB    | 08JAN01 | -25,8        | + - 0.0009       |
| HARB    | 08JAN02 | -25,8        | + - 0.0009       |
| HARB    | 08JAN08 | -25,8        | + - 0.0010       |
| HARB    | 08JAN09 | -25,8        | + - 0.0009       |
| HARB    | 08JAN10 | -25,8        | + - 0.0009       |
| HARB    | 08JAN11 | -25,8        | + - 0.0009       |
| HARB    | 08JAN12 | -25,8        | + - 0.0009       |
| HARB    | 08JAN13 | -25,8        | + - 0.0009       |
| HARB    | 08JAN14 | -25,8        | + - 0.0009       |
| HARB    | 08JAN15 | -25,8        | + - 0.0009       |

Table 7.4. Longitude coordinate files

| Site ID | Date    | Longitude(°) | Formal Error(m) |
|---------|---------|--------------|-----------------|
| HARB    | 08JAN01 | 27,7         | + - 0.0019      |
| HARB    | 08JAN02 | 27,7         | + - 0.0019      |
| HARB    | 08JAN08 | 27,7         | + - 0.0025      |
| HARB    | 08JAN09 | 27,7         | + - 0.0022      |
| HARB    | 08JAN10 | 27,7         | + - 0.0021      |
| HARB    | 08JAN11 | 27,7         | + - 0.0020      |
| HARB    | 08JAN12 | 27,7         | + - 0.0023      |
| HARB    | 08JAN13 | 27,7         | + - 0.0021      |
| HARB    | 08JAN14 | 27,7         | + - 0.0020      |
| HARB    | 08JAN15 | 27,7         | + - 0.0019      |

Table 7.5. Ellipsoidal height coordinate files

| Site ID | Date    | Ellipsoidal Height (m) | Formal Error (m) |
|---------|---------|------------------------|------------------|
| HARB    | 08JAN01 | 1558,0                 | + - 0.0041       |
| HARB    | 08JAN02 | 1561,2                 | + - 0.0041       |
| HARB    | 08JAN08 | 1561,2                 | + - 0.0049       |
| HARB    | 08JAN09 | 1561,2                 | + - 0.0044       |
| HARB    | 08JAN10 | 1561,2                 | + - 0.0042       |
| HARB    | 08JAN11 | 1561,2                 | + - 0.0041       |
| HARB    | 08JAN12 | 1561,2                 | + - 0.0042       |
| HARB    | 08JAN13 | 1561,2                 | + - 0.0042       |
| HARB    | 08JAN14 | 1561,2                 | + - 0.0040       |
| HARB    | 08JAN15 | 1561,2                 | + - 0.0041       |

At first, we cleaned results from outliers / gross errors then least squares method was used to model the accuracy of GPS PPP solutions. 3-D coordinates from short session were compared with the mean of their solutions from 24 hours data for each station and each observation session. In the end, we obtained RMS values for each side and each value of  $T$  shown in Table 7.6 - Table 7.16 computed into latitude ( $\varphi$ ), longitude ( $\lambda$ ) and ellipsoidal height ( $h$ ) components in metric units. For the precision of mathematical computations we used Excel to obtain root mean squares (RMSs) and standard deviation values in meter level accuracy.

Our stations are investigated for providing accurate 3-D positions. The duration of observation sessions varies between 1 h and 24 h. Assuming that the RMS values in Table 6.6- Table 6.16 closely approximate corresponding standard errors, we used these values to compute LS estimates for the constants:  $a_n, b_n, c_n, d_n, a_e, b_e, c_e, d_e, a_u, b_u, d_u$ .

As expected, these tables indicate that RMS values decrease as observation session increases. More to the point, ocean tide loading effect was eliminated by using Schernek's model at <http://www.oso.chalmers.se/~loading>. In the end, RMS results show that the dependency of accuracy on  $T$  is significant.

Table 7.6. BOGT RMS values for latitude, longitude, and ellipsoidal height

| BOGT | LON (m) | LAT (m) | ELLIP. HEIGHT (m) |
|------|---------|---------|-------------------|
| 01   | 0,1125  | 0,0240  | 0,1089            |
| 02   | 0,0617  | 0,0144  | 0,0676            |
| 03   | 0,0291  | 0,0065  | 0,0372            |
| 04   | 0,0176  | 0,0042  | 0,0277            |
| 06   | 0,0106  | 0,0031  | 0,0114            |
| 08   | 0,0080  | 0,0023  | 0,0107            |
| 12   | 0,0049  | 0,0020  | 0,0073            |
| 24   | 0,0022  | 0,0012  | 0,0054            |

Table 7.7. YELL RMS values for latitude, longitude, and ellipsoidal height

| YELL | LON (m) | LAT (m) | ELLIP. HEIGHT (m) |
|------|---------|---------|-------------------|
| 01   | 0,0352  | 0,0207  | 0,0452            |
| 02   | 0,0198  | 0,0093  | 0,0234            |
| 03   | 0,0144  | 0,0060  | 0,0141            |
| 04   | 0,0082  | 0,0047  | 0,0114            |
| 06   | 0,0055  | 0,0036  | 0,0060            |
| 08   | 0,0036  | 0,0023  | 0,0063            |
| 12   | 0,0029  | 0,0022  | 0,0045            |
| 24   | 0,0024  | 0,0013  | 0,0032            |

Table 7.8. HARB RMS values for latitude, longitude, and ellipsoidal height

| HARB | LON (m) | LAT (m) | ELLIP. HEIGHT (m) |
|------|---------|---------|-------------------|
| 01   | 0,0711  | 0,0265  | 0,0879            |
| 02   | 0,0286  | 0,0120  | 0,0423            |
| 03   | 0,0146  | 0,0080  | 0,0265            |
| 04   | 0,0130  | 0,0069  | 0,0179            |
| 06   | 0,0066  | 0,0035  | 0,0094            |
| 08   | 0,0051  | 0,0035  | 0,0056            |
| 12   | 0,0031  | 0,0034  | 0,0046            |
| 24   | 0,0030  | 0,0031  | 0,0032            |

Table 7.9. GUAM RMS values for latitude, longitude, and ellipsoidal height

| GUAM | LON (m) | LAT (m) | ELLIP. HEIGHT (m) |
|------|---------|---------|-------------------|
| 01   | 0,1004  | 0,0368  | 0,1370            |
| 02   | 0,0504  | 0,0141  | 0,0550            |
| 03   | 0,0308  | 0,0094  | 0,0409            |
| 04   | 0,0196  | 0,0083  | 0,0331            |
| 06   | 0,0131  | 0,0060  | 0,0233            |
| 08   | 0,0075  | 0,0040  | 0,0177            |
| 12   | 0,0066  | 0,0032  | 0,0112            |
| 24   | 0,0032  | 0,0027  | 0,0102            |

Table 7.10. MCM4 RMS values for latitude, longitude, and ellipsoidal height

| MCM4 | LON (m) | LAT (m) | ELLIP. HEIGHT (m) |
|------|---------|---------|-------------------|
| 01   | 0,0230  | 0,0848  | 0,0808            |
| 02   | 0,0139  | 0,0248  | 0,0370            |
| 03   | 0,0102  | 0,0158  | 0,0281            |
| 04   | 0,0097  | 0,0108  | 0,0196            |
| 06   | 0,0068  | 0,0071  | 0,0161            |
| 08   | 0,0053  | 0,0068  | 0,0104            |
| 12   | 0,0051  | 0,0050  | 0,0097            |
| 24   | 0,0047  | 0,0032  | 0,0079            |

Table 7.11. MALI RMS values for latitude, longitude, and ellipsoidal height

| MALI | LON (m) | LAT (m) | ELLIP. HEIGHT (m) |
|------|---------|---------|-------------------|
| 01   | 0,1050  | 0,0616  | 0,1646            |
| 02   | 0,0519  | 0,0256  | 0,0516            |
| 03   | 0,0226  | 0,0126  | 0,0377            |
| 04   | 0,0166  | 0,0140  | 0,0318            |
| 06   | 0,0100  | 0,0064  | 0,0292            |
| 08   | 0,0088  | 0,0045  | 0,0196            |
| 12   | 0,0063  | 0,0029  | 0,0169            |
| 24   | 0,0029  | 0,0021  | 0,0046            |

Table 7.12. IRKT RMS values for latitude, longitude, and ellipsoidal height

| IRKT | LON (m) | LAT (m) | ELLIP. HEIGHT (m) |
|------|---------|---------|-------------------|
| 01   | 0,1501  | 0,0538  | 0,1238            |
| 02   | 0,0410  | 0,0153  | 0,0317            |
| 03   | 0,0309  | 0,0105  | 0,0296            |
| 04   | 0,0194  | 0,0071  | 0,0262            |
| 06   | 0,0138  | 0,0051  | 0,0162            |
| 08   | 0,0066  | 0,0030  | 0,0117            |
| 12   | 0,0046  | 0,0027  | 0,0081            |
| 24   | 0,0035  | 0,0009  | 0,0079            |

Table 7.13. QUIN RMS values for latitude, longitude, and ellipsoidal height

| QUIN | LON (m) | LAT (m) | ELLIP. HEIGHT (m) |
|------|---------|---------|-------------------|
| 01   | 0,1168  | 0,0408  | 0,1202            |
| 02   | 0,0681  | 0,0167  | 0,0535            |
| 03   | 0,0310  | 0,0109  | 0,0400            |
| 04   | 0,0168  | 0,0077  | 0,0380            |
| 06   | 0,0107  | 0,0065  | 0,0265            |
| 08   | 0,0079  | 0,0055  | 0,0239            |
| 12   | 0,0062  | 0,0049  | 0,0187            |
| 24   | 0,0073  | 0,0041  | 0,0120            |

Table 7.14. RIGA RMS values for latitude, longitude, and ellipsoidal height

| RIGA | LON (m) | LAT (m) | ELLIP. HEIGHT (m) |
|------|---------|---------|-------------------|
| 01   | 0,0756  | 0,0250  | 0,0621            |
| 02   | 0,0227  | 0,0100  | 0,0275            |
| 03   | 0,0103  | 0,0049  | 0,0191            |
| 04   | 0,0056  | 0,0020  | 0,0146            |
| 06   | 0,0064  | 0,0022  | 0,0115            |
| 08   | 0,0049  | 0,0018  | 0,0132            |
| 12   | 0,0025  | 0,0016  | 0,0095            |
| 24   | 0,0013  | 0,0012  | 0,0077            |

Table 7.15. MORP RMS values for latitude, longitude, and ellipsoidal height

| MORP | LON (m) | LAT (m) | ELLIP. HEIGHT (m) |
|------|---------|---------|-------------------|
| 01   | 0,2212  | 0,0624  | 0,1122            |
| 02   | 0,0380  | 0,0177  | 0,0472            |
| 03   | 0,0148  | 0,0083  | 0,0280            |
| 04   | 0,0100  | 0,0053  | 0,0202            |
| 06   | 0,0094  | 0,0035  | 0,0109            |
| 08   | 0,0057  | 0,0026  | 0,0137            |
| 12   | 0,0040  | 0,0023  | 0,0078            |
| 24   | 0,0020  | 0,0015  | 0,0054            |

Table 7.16. SFER RMS values for latitude, longitude, and ellipsoidal height

| SFER | LON (m) | LAT (m) | ELLIP. HEIGHT (m) |
|------|---------|---------|-------------------|
| 01   | 0,2531  | 0,0553  | 0,0890            |
| 02   | 0,0575  | 0,0255  | 0,0563            |
| 03   | 0,0137  | 0,0063  | 0,0332            |
| 04   | 0,0083  | 0,0040  | 0,0207            |
| 06   | 0,0054  | 0,0039  | 0,0142            |
| 08   | 0,0044  | 0,0018  | 0,0130            |
| 12   | 0,0028  | 0,0014  | 0,0065            |
| 24   | 0,0010  | 0,0008  | 0,0014            |

For the least squares analysis, we need to arrange GPS stations in an order. Eckl *et al.*, (2001) achieves this using baseline length. Station pairs (*i.e.* baselines) are ordered from the smallest distance to the longest one. In our case, we did not carried out baseline processing as mentioned in the earlier sections. In other words, we applied Precise Point Positioning (*i.e.* absolute positioning precise clocks and orbits). Hence, we did the ordering with respect to latitude. Our motivation doing that was to see whether RMS values grow as the station latitude approaches to zero (*i.e.* equatorial latitudes). In other words, whether remaining ionospheric errors on short observing sessions affect the vertical component or not. If Table 7.17 is examined closely, one will notice that RMS errors grow as the latitude value approaches to zero.

Table 7.17. Sample of high correlation between latitude and height component

| Site ID | Latitude (°) | Height RMS (cm) |     |     |
|---------|--------------|-----------------|-----|-----|
|         |              | 1h              | 2h  | 3h  |
| MCM4    | -77,8        | 8,1             | 3,7 | 2,8 |
| HARB    | -25,9        | 8,8             | 4,2 | 2,6 |
| MALI    | -3,0         | 16,5            | 5,1 | 3,7 |
| BOGT    | 4,6          | 10,9            | 6,7 | 3,7 |
| GUAM    | 13,6         | 13,8            | 5,5 | 4,0 |
| SFER    | 36,5         | 8,9             | 5,6 | 3,3 |
| QUIN    | 40,0         | 12,2            | 5,3 | 4   |
| IRKT    | 52,2         | 12,4            | 3,1 | 2,9 |
| MORP    | 55,2         | 11,2            | 4,7 | 2,8 |
| RIGA    | 56,9         | 6,21            | 2,7 | 1,9 |
| YELL    | 62,5         | 4,52            | 2,3 | 1,4 |

For constructing the design matrix for LS analysis we used the following ordering of the GPS stations as presented in Table 7.18. It lists height RMS values with respect to latitude for 2 hours observation sessions.

Table 7.18. The ordering of stations from small to high latitude values

| Site ID | Latitude (°) | Height RMS (cm) |
|---------|--------------|-----------------|
| MALI    | 3,0          | 5,2             |
| BOGT    | 4,6          | 6,8             |
| GUAM    | 13,6         | 5,5             |
| HARB    | 25,9         | 4,23            |
| SFER    | 36,5         | 5,6             |
| QUIN    | 40,0         | 5,35            |
| IRKT    | 52,2         | 3,17            |
| MORP    | 55,2         | 4,72            |
| RIGA    | 56,9         | 2,75            |
| YELL    | 62,5         | 2,34            |
| MCM4    | 77,8         | 3,7             |

Table 7.19 summarizes the RMS errors for the component latitude. Figure 7.1 immediately reveals that 1 hour data has the largest RMS errors among the eight observation sessions.

Table 7.19. RMS values for each station for latitude component

| Station | Latitude (°) | RMS (mm) |      |      |      |
|---------|--------------|----------|------|------|------|
|         |              | 1 h      | 2 h  | 3 h  | 4 h  |
| MALI    | 3,0          | 61,6     | 25,6 | 12,6 | 14,0 |
| BOGT    | 4,6          | 24,0     | 14,4 | 6,5  | 4,2  |
| GUAM    | 13,6         | 36,8     | 14,1 | 9,4  | 8,3  |
| HARB    | 25,9         | 26,5     | 12,0 | 8,0  | 6,9  |
| SFER    | 36,5         | 55,3     | 25,5 | 6,31 | 4,0  |
| QUIN    | 40,0         | 40,8     | 16,7 | 10,9 | 7,7  |
| IRKT    | 52,2         | 53,8     | 15,3 | 10,5 | 7,1  |
| MORP    | 55,2         | 62,4     | 17,7 | 8,3  | 5,3  |
| RIGA    | 56,9         | 25,0     | 10,0 | 4,9  | 2,0  |
| YELL    | 62,5         | 20,7     | 9,37 | 6,0  | 4,7  |
| MCM4    | 77,8         | 84,8     | 24,8 | 15,8 | 10,8 |

Table 7.19. RMS values for each station for latitude component (continued)

| Station | Latitude (°) | RMS (mm) |     |      |      |
|---------|--------------|----------|-----|------|------|
|         |              | 6 h      | 8 h | 12 h | 24 h |
| MALI    | 3,0          | 6,4      | 4,5 | 2,9  | 2,1  |
| BOGT    | 4,6          | 3,1      | 2,3 | 2,0  | 1,2  |
| GUAM    | 13,6         | 6,0      | 4,0 | 3,2  | 2,7  |
| HARB    | 25,9         | 3,5      | 3,5 | 3,4  | 3,1  |
| SFER    | 36,5         | 3,9      | 1,8 | 1,4  | 0,8  |
| QUIN    | 40,0         | 6,5      | 5,5 | 4,9  | 4,1  |
| IRKT    | 52,2         | 5,1      | 3,0 | 2,7  | 0,9  |
| MORP    | 55,2         | 3,5      | 2,6 | 2,3  | 1,5  |
| RIGA    | 56,9         | 2,2      | 1,8 | 1,6  | 1,2  |
| YELL    | 62,5         | 3,6      | 2,3 | 2,2  | 1,3  |
| MCM4    | 77,8         | 7,1      | 6,8 | 5,0  | 3,2  |

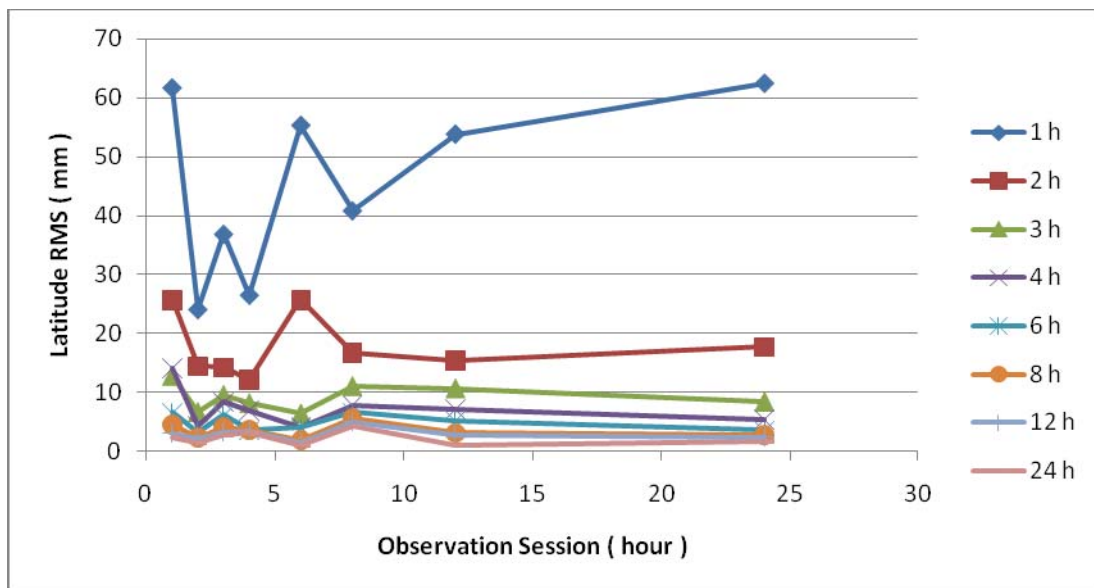


Figure 7.4. RMS values for each station for latitude component

As seen from Figure 7.4 the duration of observation sessions varies between 1 hour and 24 hours. For stations all stations, 1 hour data is considered the worst while 24 hours is considered the best solutions.

Table 7.20 summarizes the RMS values for the component longitude. From Table 7.20 and Figure 7.5 it is easy to note that the accuracy for the northward (*i.e.* latitudinal) component is better than the eastward (longitudinal) component (see also Table 7.19).

Table 7.20. RMS values for each station for longitude component

| Station | Latitude (°) | RMS (mm) |      |      |      |
|---------|--------------|----------|------|------|------|
|         |              | 1 h      | 2 h  | 3 h  | 4 h  |
| MALI    | 3,0          | 105,0    | 51,9 | 22,6 | 16,6 |
| BOGT    | 4,6          | 112,5    | 61,7 | 29,1 | 17,6 |
| GUAM    | 13,6         | 100,4    | 50,  | 30,8 | 19,6 |
| HARB    | 25,9         | 71,1     | 28,6 | 14,6 | 13,0 |
| SFER    | 36,5         | 253,1    | 57,5 | 13,7 | 8,3  |
| QUIN    | 40,0         | 116,8    | 68,1 | 31,0 | 16,8 |
| IRKT    | 52,2         | 150,1    | 41,0 | 30,9 | 19,4 |
| MORP    | 55,2         | 221,2    | 38,0 | 14,8 | 10,0 |
| RIGA    | 56,9         | 75,6     | 22,7 | 10,3 | 5,6  |
| YELL    | 62,5         | 35,2     | 19,8 | 14,4 | 8,2  |
| MCM4    | 77,8         | 23,0     | 13,9 | 10,2 | 9,7  |

Table 7.20. RMS values for each station for longitude component (continued)

| Station | Latitude (°) | RMS (mm) |     |      |      |
|---------|--------------|----------|-----|------|------|
|         |              | 6 h      | 8 h | 12 h | 24 h |
| MALI    | 3,0          | 10,0     | 8,8 | 6,3  | 2,9  |
| BOGT    | 4,6          | 10,6     | 8,0 | 4,9  | 2,2  |
| GUAM    | 13,6         | 13,1     | 7,5 | 6,6  | 3,2  |
| HARB    | 25,9         | 6,6      | 5,1 | 3,1  | 3,0  |
| SFER    | 36,5         | 5,4      | 4,4 | 2,8  | 1,0  |
| QUIN    | 40,0         | 10,7     | 7,9 | 6,2  | 7,3  |
| IRKT    | 52,2         | 13,8     | 6,6 | 4,6  | 3,5  |
| MORP    | 55,2         | 9,4      | 5,7 | 4,0  | 2,0  |
| RIGA    | 56,9         | 6,4      | 4,9 | 2,5  | 1,3  |
| YELL    | 62,5         | 5,       | 3,  | 2,9  | 2,4  |

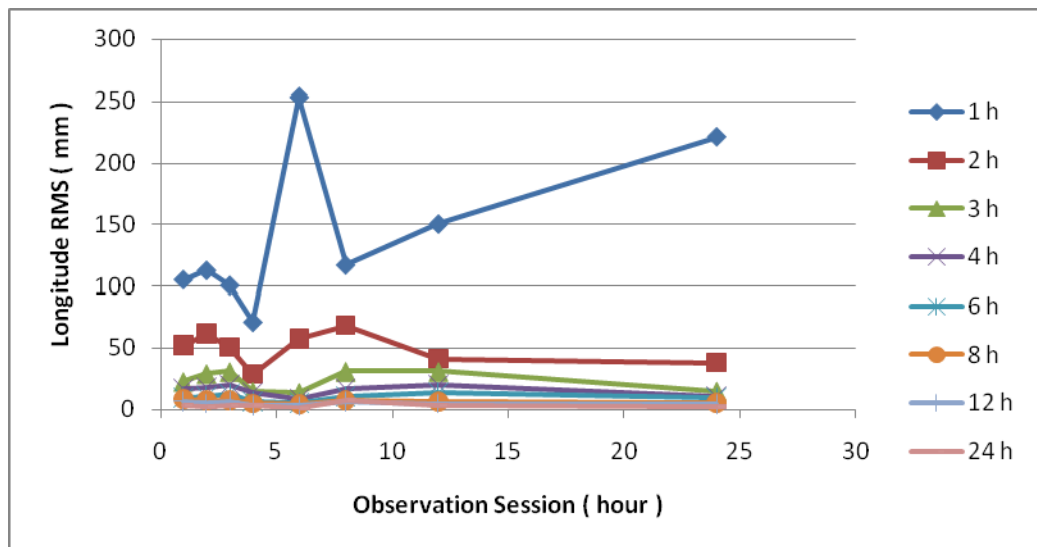


Figure 7.5. RMS values for each station for longitude component

Table 7.21 summarizes RMS values for the ellipsoidal height component. Graphical representation of Table 7.21 is given in Figure 7.6. As will be noticed, the RMSs of height are the worst of all three GPS components (see also Table 7.19 and 7.20).

Table 7.21. RMS values for each station for ellipsoidal height component

| Station | Latitude<br>(°) | RMS (mm) |      |      |      |      |      |      |      |
|---------|-----------------|----------|------|------|------|------|------|------|------|
|         |                 | 1 h      | 2 h  | 3 h  | 4 h  | 6 h  | 8 h  | 12 h | 24 h |
| MALI    | 3,0             | 164,6    | 51,6 | 37,7 | 31,8 | 29,2 | 19,6 | 16,9 | 4,6  |
| BOGT    | 4,6             | 108,9    | 67,6 | 37,2 | 27,7 | 11,4 | 10,7 | 7,3  | 5,4  |
| GUAM    | 13,6            | 137      | 55   | 40,9 | 33,1 | 23,3 | 17,7 | 11,2 | 10,2 |
| HARB    | 25,9            | 87,9     | 42,3 | 26,5 | 17,9 | 9,4  | 5,6  | 4,6  | 3,2  |
| SFER    | 36,5            | 89       | 56,3 | 33,2 | 20,7 | 14,2 | 13   | 6,5  | 1,4  |
| QUIN    | 40,0            | 120,2    | 53,5 | 40   | 38   | 26,5 | 23,9 | 18,7 | 12   |
| IRKT    | 52,2            | 123,8    | 31,7 | 29,6 | 26,2 | 16,2 | 11,7 | 8,1  | 7,9  |
| MORP    | 55,2            | 112,2    | 47,2 | 28   | 20,2 | 10,9 | 13,7 | 7,8  | 5,4  |
| RIGA    | 56,9            | 62,1     | 27,5 | 19,1 | 14,6 | 11,5 | 13,2 | 9,5  | 7,7  |
| YELL    | 62,5            | 45,2     | 23,4 | 14,1 | 11,4 | 6    | 6,3  | 4,5  | 3,2  |
| MCM4    | 77,8            | 80,8     | 37   | 28,1 | 19,6 | 16,1 | 10,4 | 9,7  | 7,9  |

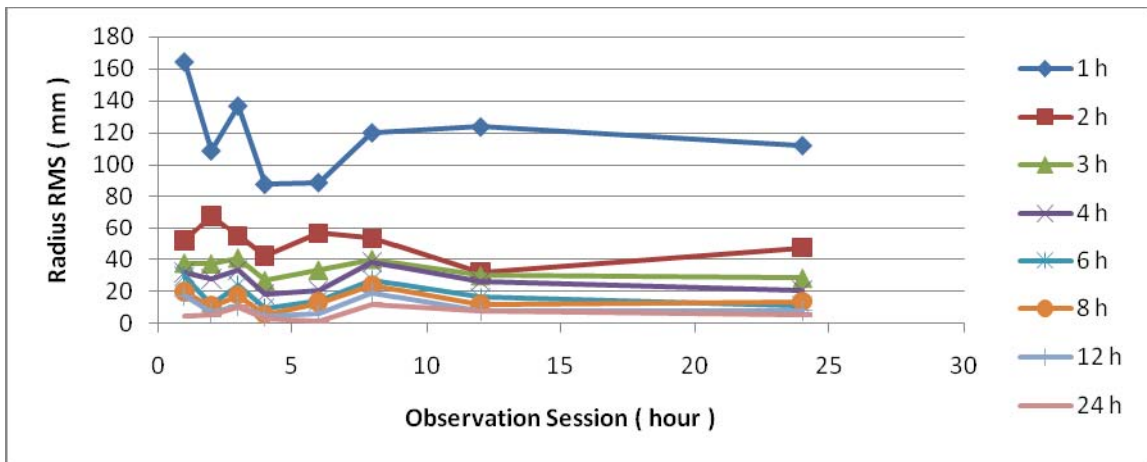


Figure 7.6. RMS values for each station for radius component

## 8. ACCURACY ANALYSIS

For the estimation of the components latitude, longitude, and ellipsoidal height we used standard deviation expression given by Eckl *et al.*, (2001). In there, time is inversely proportional to  $a$  and  $b$  while latitude is proportional to  $b$  and  $d$  values.  $c$  is the constant which is independent of  $T$  and  $\varphi$ . The representation of our equations of standard deviations is  $S_e(\varphi, T)$ ,  $S_n(\varphi, T)$  and  $S_u(\varphi, T)$  which are longitude, latitude, and ellipsoidal height (radius) respectively.

$$S_e(\varphi, T) = \sqrt{\frac{a_e}{T} + \frac{(b_e \times \varphi^2)}{T} + c_e + d_e \times \varphi^2} \quad (8.1)$$

$$S_n(\varphi, T) = \sqrt{\frac{a_n}{T} + \frac{(b_n \times \varphi^2)}{T} + c_n + d_n \times \varphi^2} \quad (8.2)$$

$$S_u(\varphi, T) = \sqrt{\frac{a_u}{T} + \frac{(b_u \times \varphi^2)}{T} + c_u + d_u \times \varphi^2} \quad (8.3)$$

Using the RMS values given in Tables 7.19 through 7.21 the design matrix was formed. Then the unknown parameters  $a_n$ ,  $a_e$ ,  $a_u$ ;  $b_n$ ,  $b_e$ ,  $b_u$ ; and  $c_n$ ,  $c_e$ ,  $c_u$  were obtained. Applying Student's  $t$  test, we determined statistically significant parameters. The results show that in the end of computations of matrixes, a simple formulation with only the coefficient ' $a$ ' was possible. Therefore, as seen from the equations (8.6), (8.7), and (8.8) the dependency of accuracy on time is significant.

$$\text{Se}(\varphi, T) = \sqrt{\frac{a_c}{T}} \quad (8.5)$$

$$\text{Sn}(\varphi, T) = \sqrt{\frac{a_n}{T}} \quad (8.6)$$

$$\text{Su}(\varphi, T) = \sqrt{\frac{a_u}{T}} \quad (8.7)$$

Our stations were investigated for providing accurate 3-D positions and the dependency of accuracy on  $T$  has been found to be significant:

$$\text{Sn}(T) = \sqrt{\frac{182,11}{T}} = 13,5/\sqrt{T} \quad (8.8)$$

$$\text{Se}(T) = \sqrt{\frac{428,72}{T}} = 20,7/\sqrt{T} \quad (8.9)$$

$$\text{Su}(T) = \sqrt{\frac{1668,90}{T}} = 40,8/\sqrt{T} \quad (8.10)$$

Using the formulas given 8.8 through 8.10 we predicted GPS accuracies and then compared them with the RMS values given in Tables 7.19 through 7.21. The modified empirical formula first presented in Eckl *et al.* (2001) shown in equation (8.1) gives negative value when the observation span was reduced to less than 6 h. As seen from the Table 8.1 only the RMS values from 6 hours or longer observation sessions can be used to derive prediction formulas. In Table 8.1, the mean RMS values of the GPS PPP solutions

derived from Tables 7.19 through 7.21 are also given in brackets. Comparison with the accuracy prediction using the equations 8.8 through 8.10 agrees at 1 mm level on average.

Table 8.1. Comparing accuracy prediction with the mean RMS of GPS PPP solutions

| Hour | Latitude (mm) | Longitude (mm) | Radius (mm) |
|------|---------------|----------------|-------------|
| 6    | 5,5 (4.7)     | 8,4 (9.0)      | 16,6 (15.9) |
| 8    | 4,8 (3.5)     | 7,3 (6.2)      | 14,4 (13.2) |
| 12   | 3,9 (2.9)     | 6,0 (4.5)      | 11,8 (9.5)  |
| 24   | 2,8 (2.1)     | 4,2 (3.1)      | 8,3 (6.3)   |

We also compared our prediction results with the PPP results given in Tsakiri 2008. Tsakiri (2008) compared GPS results from various online PPP software and the software Auto-GIPSY is also included in the assessment. The comparison is given in Table 8.2. There the RMS values in brackets imply average of the RMS values calculated from the processing of Tsakiri (2008).

Table 8.2. Comparing our PPP results with online Auto-GIPSY results

| Hour | Latitude (mm) | Longitude (mm) | Radius (mm) |
|------|---------------|----------------|-------------|
| 6    | 5,5 (14.6)    | 8,4 (15.9)     | 16,6 (25.0) |
| 24   | 2,8 (6.4)     | 4,2 (16.0)     | 8,3 (14,6)  |

One can infer from Table 8.2 that Auto-GIPSY results are coarser compared to our GIPSY PPP results.

## 9. CONCLUSIONS

Positioning with GPS can be performed by either of two ways: point positioning or differential (relative) positioning. GPS point positioning employs one GPS receiver, while differential positioning employs two (or more) GPS receivers simultaneously tracking the same satellites. New developments in GPS positioning and our findings here show that a user with a single GPS receiver can obtain positioning accuracy comparable to that of differential positioning

Our results indicate that the formulation of the accuracy of GPS PPP shows similarity with the formulation of the accuracy of GPS relative positioning. Namely, the accuracy depends only on the observing session duration  $T$ .

A minimum of 6 hours of data is recommended to obtain results sufficiently accurate for surveying applications. Application of the standard deviation expression given by Eckl *et al.*, (2001) fails for observation sessions shorter than 6 hours. We suspect poor satellite-receiver geometry, second order ionospheric effects and multipath play an important role in our GPS solutions. We actually detected dependency on latitude for the solutions of GPS vertical positioning. At equatorial latitudes RMS errors grow larger for vertical positioning. However, the dependency on latitude changes when observation span extended longer than 5 hours.

Although similar data sampling and processing strategies are applied, on line Auto-GIPSY results are far less accurate than our conventional GIPSY processing results. Tsakiri (2008) ascribes this to the fact “online processing services are not regulated to some standard and the solutions provided have no form of guaranteed quality”. Obviously this conclusion requires detailed investigation be conducted in the field.

## REFERENCES

- Altamimi, Z., X. Collilieux, J. Legrand, B. Garayt, and C. Boucher, 2007, "ITRF2005: A new release of the International Terrestrial Reference Frame based on time series of station positions and Earth Orientation Parameters", *Journal of Geophysical Research*, Vol. 112, No. 1, pp. 41-48.
- Blewitt, G., 1997, "Basics of the GPS Technique: Observation Equations", *Geodetic Applications of GPS*, Swedish Land Survey.
- Blewitt, G., 1997, *GPS Technology*, <http://www.gisdevelopment.net/technology/gps/ma04123a.htm>.
- Dogan, U., 2007, "Accuracy Analysis of Relative Positions of Permanent GPS Stations in the Marmara Region, Turkey", *Survey Review*, Vol. 39 (304), pp. 156-165.
- Eckl, M.C., R.A. Snay, T. Soler, M.W. Cline and G.L. Mader, 2001, "Accuracy of GPS-derived Relative Position as a Function of Inter-station Distance and Observing Session Duration", *Journal of Geodesy*, Vol. 75, pp. 633-640.
- El-Rabbany, A., 2002, "Introduction to GPS: the Global Positioning System", *Ahmed Artech House*.
- Heflin, M. B., 2009, *GPS Products*, [http://www.geod.nrcan.gc.ca/products-produits/eph\\_e.php](http://www.geod.nrcan.gc.ca/products-produits/eph_e.php).
- IERS, 2009, *GPS Sites*, <http://www.iers.org>.
- Jursa, A. S., 1985, "Handbook of Geophysics and the Space Environment". Air Force Geophysics Laboratory, National Technical Information Services, Springfield, Virginia.

- King, M., S. Edwards and P. Clarke, 2002, Precise Point Positioning: Breaking the Monopoly of Relative GPS Processing, *Engineering Surveying*.
- Langley, R., 1991, "The Mathematics of GPS.", *GPS World*, Vol. 2, No. 7, pp. 45-50.
- McCarthy, D.D. and G. Petit, 2003, *IERS Conventions, IERS Technical Note 32*, Int. Earth Rotation Serv., Paris.
- Mendes, V.B., and R.B. Langley, 2000, "An analysis of high-accuracy tropospheric delay mapping functions", *Physics and Chemistry of the Earth*, Vol. 25, No. 12, pp. 809-812.
- Menge, F., 2008, *GPS Technique* , <http://www.gportal.it/igsframeset.php>.
- Nasa, 2009, *GPS Technology*, <http://igscb.jpl.nasa.gov/network/complete.html>.
- Saastamoinen, J., 1972, "Atmospheric correction for the troposphere and stratosphere in radio ranging of satellites", *The Use of Artificial Satellites for Geodesy*, pp. 247–251.
- Sanli, D. U. and F. Kurumahmut, 2008, "Accuracy of GPS Positioning in the Presence of Large Height Differences," *FIG Working Week 2008*, Stockholm-Sweden.
- Sherneck, H. and M. Bos, 2000, Ocean Tide and Atmospheric Loading, <http://www.oso.chalmers.se/~loading>.
- Scherneck, H. G. and F. H. Webb., 1998a, "Ocean Tide Loading and Diurnal Tidal Motion of the Solid Earth Center", *IERS Technical Note*, Vol. 3, No. 25, pp. 48-50.
- Stewart, M. P., 1998, "The application of antenna phase center models to the west Australian state GPS network" *Geodetic Applications of GPS*, Swedish Land Survey.

- Stewart, M. P., 1998, *The application of antenna phase center models*,  
<http://www.garmin.com/aboutGPS>.
- Townsend, B. R. and P. Fenton, 1994, "A Practical Approach to the Reduction of Pseudorange Multipath Errors in a L1 GPS Receiver", *Proceedings of the 7th International Technical Meeting of the Satellite Division of the Institute of Navigation*, Salt Lake City, UT, USA.
- Townsend, B. R. and P. Fenton, 1995, "L1 Carrier Phase Multipath Error Reduction Using MEDLL Technology".
- Witchayangkoon, B., 2000, *Elements of GPS Precise Point Positioning*, The University of Maine the Degree of Doctor of Philosophy.
- Wubbena, G., M. Schmitz, F. Menge and G. Seeber, 1997, "A New Approach for Field Calibration of Absolute GPS Antenna Phase Center Variations", *Navigation: J. the Inst. of Navigation*, Vol. 44 (Ed.2), Summer, pp. 247-255.
- VanDam, T.M., G. Blewitt, and M.B. Heflin, 1994, "Atmospheric Pressure Loading Effects on Global Positioning System Coordinate Determinations", *Journal of Geophysical research*, Vol. 99, B12, 23,939-23,950.
- Yavasoglu, 1997, *GPS Technique*,  
[http://www.atlas.cc.itu.edu.tr/~yavasoglu/GPS\\_technique/GPS\\_Tech\\_06.ppt](http://www.atlas.cc.itu.edu.tr/~yavasoglu/GPS_technique/GPS_Tech_06.ppt).
- Zumberge, J. F., M. B. Heflin, D. C. Jefferson, M. M. Watkins and F. H. Webb, 1997, "Precise Point Positioning for the efficient and robust analysis of GPS data from large networks", *Journal of Geophysical Research*, Vol. 102, pp. 5005-5018.

## **AUTOBIOGRAPHY**

Simge Tekiç

Bogazici University, Turkey

She was born in 1984 at İstanbul. In 2006 she got his B.S. degree in Geodesy and Photogrammetry Engineering from Yıldız Technical University. She is a member of the Turkish Chamber of Surveying Engineers